NACA

RESEARCH MEMORANDUM

FORCE AND PRESSURE RECOVERY CHARACTERISTICS AT

SUPERSONIC SPEEDS OF A CONICAL SPIKE INLET WITH

A BYPASS DISCHARGING FROM THE TOP OR BOTTOM

OF THE DIFFUSER IN AN AXIAL DIRECTION

By J. L. Allen and Andrew Beke

Lewis Flight Propulsion Laboratory
Cleveland, Ohio

NATIONAL ADVISORY COMMITTEE
FOR AERONAUTICS
WASHINGTON

March 23, 1953
Declassified October 28, 1960

NATIONAL ADVISORY COMMITTEE FOR AERONAUTICS

RESEARCH MEMORANDUM

FORCE AND PRESSURE RECOVERY CHARACTERISTICS AT SUPERSONIC

SPEEDS OF A CONICAL SPIKE INLET WITH A BYPASS

DISCHARGING FROM THE TOP OR BOTTOM OF THE

DIFFUSER IN AN AXIAL DIRECTION

By J. L. Allen and Andrew Beke

SUMMARY

An axially symmetric nacelle-type conical spike inlet with a fixed-area bypass located in the top or bottom of the diffuser was investigated in the Lewis 8- by 6-foot supersonic tunnel. The bypass was sized to discharge in a nearly axial direction about 10 percent of the maximum mass flow captured by the inlet. Force and pressure recovery data were obtained at flight Mach numbers of 1.6, 1.8, and 2.0 over a range of angles of attack from 0° to 9°.

Top or bottom location of the bypass within the diffuser did not have significant effects on diffuser pressure recovery, bypass mass-flow ratio, or drag coefficient over the range of angles of attack, flight Mach numbers, and stable engine mass-flow ratios investigated. At a flight Mach number of 2.0 and angles of attack from 3° to 9°, a larger stable subcritical operating range was obtained with the bypass on the bottom. Higher lift coefficients and more positive pitching moments were obtained with the bypass on the bottom over the range of angles of attack and flight Mach numbers investigated.

At zero angle of attack and a flight Mach number of 2.0, about 14 percent of the maximum stream tube entering the inlet was bypassed with a drag increase of only 20 percent of the additive drag that would result for equivalent spillage behind an inlet normal shock. Diffuser total-pressure recovery was not significantly reduced compared with results obtained without bypasses.

INTRODUCTION

Previous investigations (refs. 1 and 2) of an axially symmetric spike-type nose inlet indicated that discharging mass flow in excess of engine requirements by means of a bypass increased the drag by only a

fraction of the additive drag that would result for equivalent normal-shock spillage and did not significantly reduce diffuser total-pressure recovery. The data of reference 2 were obtained with two fixed-area bypasses on opposite sides of the model in a horizontal plane, and the total mass flow bypassed was about 20 percent of the free-stream tube entering the inlet. At angles of attack other than zero, various circumferential locations of the bypass may result in significant variations in performance because of differences in the external flow field near the bypass exit as well as internal flow differences near the bypass entrance. In addition, bypass mass flows less than those of reference 2, which would be necessary for a variable mass-flow bypass system, may not result in proportional gains in performance compared with normal-shock spillage. Therefore, in order to extend the results of reference 2, the same inlet model was investigated with one identical bypass installed in the top or bottom of the diffuser. The investigation was conducted in the NACA Lewis laboratory 8- by 6-foot supersonic tunnel and the results are presented herein.

SYMBOLS

The following symbols are used in this report:

A area

A_m maximum external cross-sectional area

C_D drag coefficient, external drag plus internal and external drag
           due to bypassing mass flow, $D/q_0 A_m$

C_L lift coefficient,
           $$\frac{\text{measured lift minus internal lift due to engine mass flow}}{q_0 A_m}$$

C_M pitching-moment coefficient about base of model,
           $$\frac{\text{total minus internal pitching-moment due to engine mass flow}}{q_0 A_m l}$$

C_{T-D} thrust-minus-drag coefficient, $(T - D)/q_0 A_m$

D drag force, external drag plus internal and external drag due
           to bypassing

L length of subsonic diffuser, 46.9 in.

l over-all length of model, 58.7 in.

M   Mach number

m   mass flow

m_b/m_0 bypass mass-flow ratio, $\dfrac{\text{bypass mass flow}}{\rho_0 V_0 A_1}$

m_4/m_0 engine mass-flow ratio, $\dfrac{\text{engine mass flow}}{\rho_0 V_0 A_1}$

P   total pressure

p   static pressure

(p_s/P_j) bypass or nozzle pressure ratio, surface static pressure without bypass (station 33.0) per total pressure of jet

q   dynamic pressure, $\gamma p M^2/2$

T   thrust, net force in flight direction due to change of momentum of engine mass flow between free stream (station 0) and diffuser discharge (station 4) including balance base force

V   velocity

x   longitudinal station, in.

α nominal angle of attack, deg

γ ratio of specific heats for air

ρ mass density of air

Subscripts:

b   bypass

x   longitudinal station

0   free stream

1   leading edge of cowl

4   diffuser discharge at constant diameter section, station 46.9

4,1   diffuser discharge at constant diameter section (sting out), station 46.9

Pertinent areas:

A_m maximum external cross-sectional area, 0.360 sq ft

A_1 inlet capture area defined by cowl lip (measured), 0.155 sq ft

A_4 flow area at diffuser discharge, 0.289 sq ft

$A_{4,1}$ flow area at diffuser discharge (sting out), 0.338 sq ft

APPARATUS AND PROCEDURE

The model, which was identical to inlet B of reference 1, consisted of a single-conical-shock inlet without internal contraction, an annular subsonic diffuser, and a fixed-area bypass which was identical to the bypass of reference 2 except for circumferential location (fig. 1). Tip projection of the 25°-half-angle cone was selected so that the conical shock would intercept the leading edge of the cowl lip at a flight Mach number of 2.0 and provide a mass-flow ratio of unity. At this condition the streamline behind the oblique shock was nearly alined with the slope of the external portion of the cowl lip. Coordinates of the cowl and centerbody are presented in table I and the longitudinal area variation of the subsonic diffuser is shown in figure 2. The area ratio is expressed as the quotient of the local flow area based on the average normal to the annulus surfaces and the maximum flow area at the diffuser discharge (station 46.9). The leading edge of the bypass was approximately 6 inlet diameters downstream of the inlet entrance and corresponded to a position slightly forward of the compressor inlet of a turbojet engine or the combustion chamber of a ram-jet engine.

The bypass insert and the outer body, or shell, formed a convergent-divergent asymmetric nozzle, shown photographically in figure 3 and in detail in figure 4, which was capable of discharging in a nearly axial direction about 10 percent of the maximum mass flow captured by the inlet. The external surface of the bypass was a channel set at an angle of $3\frac{1}{2}°$ relative to the model axis of symmetry and did not protude beyond the external cylindrical contour of the model.

The model, which was sting-mounted from the tunnel strut, had an internal three-component strain-gage balance. Balance normal and moment readings were used in conjunction with a static calibration of model and sting to correct the angles of attack for deflections due to aerodynamic loads. Actual angles of attack were as much as 0.4° greater than the nominal angles; however, all data were reduced for the nominal angles of attack. Differences in actual angles of attack between the model with the bypass located on the top or bottom were

within 0.1°. Regions of inlet instability, or pulsing, were determined from time-force histories of axial-force variation and by means of high-speed schlieren motion pictures.

The sum of the mass-flow ratios of the engine and the bypass, based on the mass flow of a free-stream tube defined by the cowling capture area, is the mass-flow ratio of the inlet. Methods of instrumentation and calculation are given in reference 2. The accuracy of the engine mass-flow ratio is approximately 1 percent at zero angle of attack and within 2 percent at an angle of attack of 9°.

In order to account for the thrust developed between the plane of survey (station 36.7) and the diffuser discharge (station 46.9), the diffusion between these stations was assumed to be isentropic. The measured thrust-minus-drag coefficients correspond to diffusion with the support sting removed inasmuch as the force (determined by measuring the static pressure) acting on the base of the strain-gage balance is, within about 1 percent, equal to that obtained by diffusing isentropically from area A_4 to $A_{4,1}$. Accordingly, the diffuser-discharge Mach numbers are based on the area $A_{4,1}$. The Reynolds number, based on inlet diameter, varied from 2.10 to 2.19×10^6.

RESULTS AND DISCUSSION

Presentation of Results

The variation of bypass mass-flow ratio, total-pressure recovery, diffuser-discharge Mach number, and coefficients of thrust-minus-drag, drag, lift, and pitching-moment with engine mass-flow ratio are presented in figures 5 to 8 for the bypass mounted in the top of the diffuser and in figures 9 to 12 for the bottom bypass location. Data obtained at flight Mach numbers of 1.6, 1.8, and 2.0 are presented in figures 5 and 9 for a nominal angle of attack of zero and in figures 6 and 10 for a nominal angle of attack of 6° for the inlet with the bypass on the top and bottom, respectively. Data for nominal angles of attack of 3° and 9° at a flight Mach number of 2.0 are presented in figures 7 and 11, and lift and pitching-moment coefficients for all flight Mach numbers and angles of attack investigated are presented in figures 8 and 12. Schlieren photographs showing the flow field in the region of the bypass discharge are presented in figure 13 for the two bypass locations and angles of attack of 0° and 9°.

The thrust-minus-drag coefficients were obtained from the strain-gage balance readings and correspond to the net force on the model in the flight direction with sting removed and can be used for general comparisons of the data. Since the over-all thrust of the propulsive unit

is composed of the net forces of the inlet diffuser, engine, and exhaust nozzle, the thrust-minus-drag coefficient can be used directly in computing propulsive unit performance. Drag force was obtained by subtracting the measured thrust-minus-drag from the thrust computed from the mass flow consumed by the engine (see SYMBOLS). The drag coefficient thus includes the external drag of the model plus the net internal and external effect due to bypassing mass flow. Similarly, the lift and pitching-moment coefficients are the difference between the measured value and the computed internal lift or pitching moment caused by the engine mass flow. The additive components due to mass-flow spillage behind the inlet shock system are included in the drag, lift, and pitching-moment coefficients. Pitching-moment coefficients were computed by assuming that the turning of the engine mass flow occurred at the cowl lip.

Effect of Top or Bottom Location of Bypass

For symmetrical bodies at positive angles of attack, it has been observed that the high-energy portion of the internal flow tends to congregate in the upper portion of the diffuser (ref. 3) and that the external flow field near the afterbody is characterized by vortex cores or lobes near the upper surface and by a thinner boundary layer on the underside due to the effects of viscous crossflow (ref. 4). Differences in bypass and inlet performance might be anticipated for a bypass located in these various flow fields. In general, however, top or bottom location of the bypass had little effect on diffuser total-pressure recovery, bypass mass-flow ratio, and drag coefficient over the range of angles of attack and flight Mach numbers investigated in the region of stable inlet flow. At angles of attack from 3° to 9°, slightly lower drag coefficients were obtained for the top location of the bypass. This lower drag may be associated with the flow of the jet over the inclined upper surface.

Of particular interest is the larger stable subcritical operating range obtained with the bypass located on the bottom of the diffuser for a flight Mach number of 2.0 and angles of attack of 3°, 6°, and 9°. This is probably associated with the effects of bypassing the internal flow. For example, the lower location of the bypass may eliminate (or reduce) separated flow over the lower surface of the internal shell, whereas bypassing air from the top may increase the crossflow to the top and thus accentuate separation on the lower surface.

Lift coefficients were slightly higher and pitching-moment coefficients were more positive over the range of flight Mach numbers, angles of attack, and engine mass-flow ratios with the bypass located on the bottom of the diffuser, probably because of incremental lift resulting from turning the bypass mass flow downward at the exit and because of an effective change in body shape due to the jet (figs. 8 and 12).

At a flight Mach number of 2.0 and a nominal angle of attack of 0° (actual angle about 0.4°), the lift coefficient, compared with results obtained without bypasses, was increased 0.02 with the bypass on the bottom of the diffuser and decreased 0.015 with the bypass on the top.

Other small performance differences between top and bottom location of the bypass exist over the range of conditions investigated; however, no other consistent trends are evident.

The schlieren photographs in figure 13 indicate that the jet from the bypass was discharged behind an oblique shock wave (similar to the exit flow from a sonic symmetrical nozzle), and further, that the boundary layer of the body had been displaced in a vertical direction by the jet, a phenomena which was also observed in reference 5 where the jet was discharged normal to the surface. Losses attributed to the oblique shock could be reduced by designing the bypass nozzle to re-expand to the local exit conditions. Mixing phenomena of the jet, boundary layer, and local stream are believed to be similar to those discussed in reference 5.

Comparison With Previous Results

In an actual installation or application of a bypass system, the amount of mass flow bypassed would have to vary in order to maintain critical inlet flow over a range of engine mass-flow requirements. This could be accomplished by varying the minimum area of the bypass or by varying the number of open fixed-area bypasses; in either case the sonic discharge area would be a variable. Therefore, the critical inlet flow data obtained in this investigation, with two bypasses (ref. 2), and without bypasses (ref. 1) represent three design points which, considering first-order effects, define an envelope curve for the operating characteristics of a variable mass-flow bypass system. A comparison of these data is shown in figure 9.

At the design point of the bypass (critical inlet flow, $M_0 = 2.0$, $\alpha = 0^\circ$), the increase in drag attributed to bypassing 14 percent of the maximum mass flow captured by the inlet is only 20 percent of the additive drag that would result from equivalent mass-flow spillage behind an inlet normal shock. In reference 2, 23 percent of the critical mass flow was bypassed and the increase in drag was also 20 percent of the corresponding additive drag. At flight Mach numbers of 1.8 and 1.6, drag coefficients at critical inlet flow are somewhat higher than those obtained with two bypasses. This apparent discrepancy may be within the accuracy of measurement of the comparatively small force differences. Additional contributing factors are the small computational error in mass-flow ratio and the difficulty of accurate definition of the point of critical inlet flow.

Diffuser total-pressure recoveries were about equal to those obtained with two bypasses (ref. 2) and slightly lower than those obtained without bypasses (ref. 1).

Comparisons of the thrust-minus-drag coefficients (thus including the net effects of pressure recovery and drag) indicate that maintaining critical inlet conditions by means of a bypass increased the net force on the model in the flight direction about 4 percent over that obtained with inlet normal-shock spillage at a flight Mach number of 2.0 (fig. 9(b)). Further comparison at critical inlet flow indicates a monotonic increase in thrust-minus-drag coefficient as the bypass mass-flow ratio is increased (by addition of one and then two fixed-area bypasses to the basic inlet model) at flight Mach numbers of 2.0, 1.8, and 1.6. This increase in thrust-minus-drag is the net result of increased diffuser thrust and the drag rise due to bypassing (diffuser thrust increases because the diffuser-discharge Mach number decreases as the engine mass-flow ratio is decreased). The increase in diffuser thrust is the primary cause of the increase in thrust-minus-drag since the change in bypass drag is comparatively small.

Application of the bypass is not necessarily restricted to maintaining critical inlet flow conditions. The amount of mass flow in excess of engine requirements can be proportioned between normal-shock and bypass spillage and higher thrust-minus-drag coefficients compared with those attainable with normal-shock spillage alone can be obtained; however, this may not be so efficient as operation at critical inlet flow.

CONCLUDING REMARKS

Diffuser total-pressure recovery, bypass mass-flow ratio, and drag coefficient were not significantly affected by vertical location (top or bottom) of the bypass over the range of angles of attack, flight Mach numbers, and stable engine mass-flow ratios investigated. For angles of attack from 3^0 to 9^0 at a flight Mach number of 2.0, a larger stable subcritical operating range was obtained with the bypass on the bottom. Over the range of angles of attack and flight Mach numbers investigated, the lift coefficients were higher and pitching-moment coefficients more positive for the bottom bypass location.

At a flight Mach number of 2.0, the bypass discharged about 14 percent of the full-stream tube that entered the inlet with a drag increase of only 20 percent of the additive drag that would result for equivalent spillage behind an inlet normal shock. Diffuser total-pressure recovery was not significantly reduced compared with results obtained without a bypass.

Lewis Flight Propulsion Laboratory
    National Advisory Committee for
        Cleveland, Ohio

REFERENCES

1. Beke, Andrew, and Allen, J. L.: Force and Pressure-Recovery Characteristics of a Conical-Type Nose Inlet Operating at Mach Numbers of 1.6 to 2.0 and at Angles of Attack to 9°. NACA RM E52I30, 1952.

2. Allen, J. L., and Beke, Andrew: Force and Pressure Recovery Characteristics at Supersonic Speeds of a Conical Spike Inlet with Bypasses Discharging in an Axial Direction. NACA RM E52K14, 1952.

3. Esenwein, Fred T., and Valerino, Alfred S.: Force and Pressure Characteristics for a Series of Nose Inlets at Mach Numbers from 1.59 to 1.99. I - Conical Spike All-External Compression Inlet with Subsonic Cowl Lip. NACA RM E50J26, 1951.

4. Luidens, Roger W., and Simon, Paul C.: Aerodynamic Characteristics of NACA RM-10 Missile in 8- by 6-Foot Supersonic Wind Tunnel at Mach Numbers from 1.49 to 1.98. I - Presentation and Analysis of Pressure Measurements (Stabilizing Fins Removed). NACA RM E50D10, 1950.

5. Nelson, William J., and Dewey, Paul E.: A Transonic Investigation of the Aero-Dynamic Characteristics of Plate- and Bell-Type Outlets for Auxiliary Air. NACA RM L52H20, 1952.

TABLE I - COORDINATES

Centerbody	
Station, in.	Radius, in.
-2.86	[a]0
-.2	[a]1.24
0	1.32
.1	1.36
.2	1.39
.3	1.42
.4	1.45
.5	1.48
.8	1.56
1.0	1.61
1.5	1.73
2.0	1.84
2.5	1.92
3.0	2.01
4.0	2.14
5.0	2.24
6.0	2.31
7.0	2.37
8.0	2.42
9.0	2.44
10.0	2.46
12.0	2.46
14.0	2.44
16.0	2.40
18.0	2.32
20.0	2.19
22.4	2.03
24.0	1.95
28.0	1.75
32.0	1.61
37.1	1.50
46.9	1.50
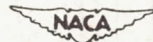
Cowling		
Station, in.	External radius, in.	Internal radius, in.
0	2.671	2.671
.015	2.686	2.656
.5	2.79	2.73
1.0	2.89	2.80
1.5	2.97	2.86
2.0	3.04	2.92
2.5	3.11	2.98
3.0	3.16	3.03
4.0	3.25	3.12
5.0	3.32	3.20
6.0	3.38	3.25
7.0	3.42	3.30
8.0	3.45	3.33
8.67	3.47	3.35

[a]Region of 25°-half-angle cone.
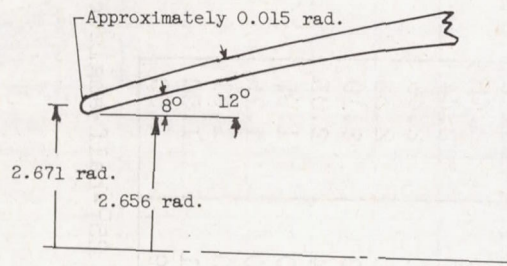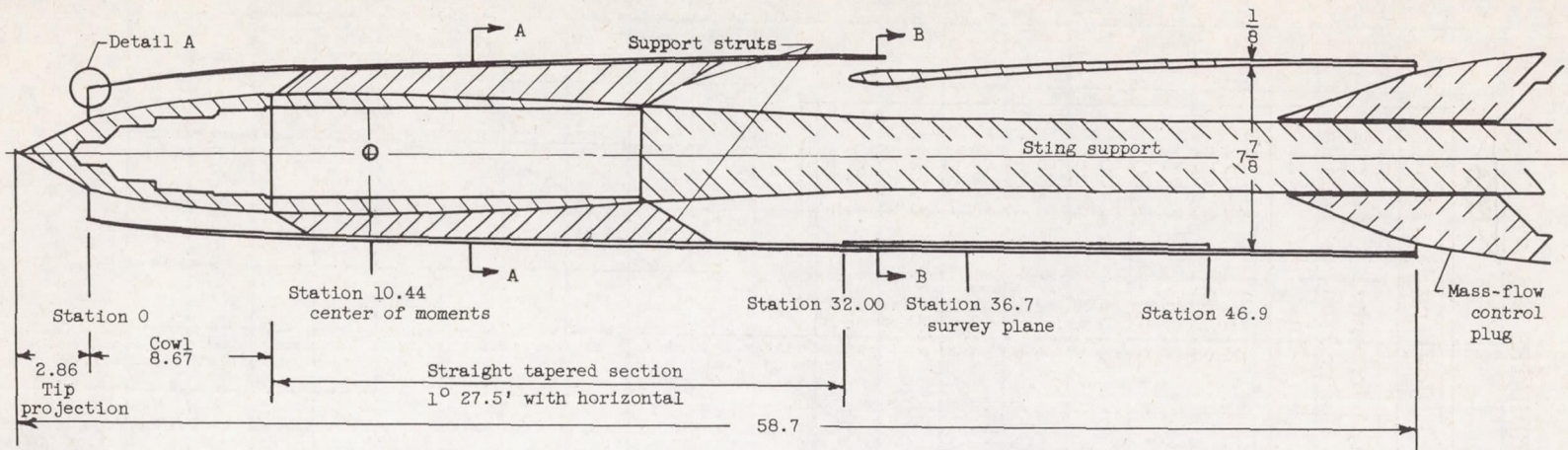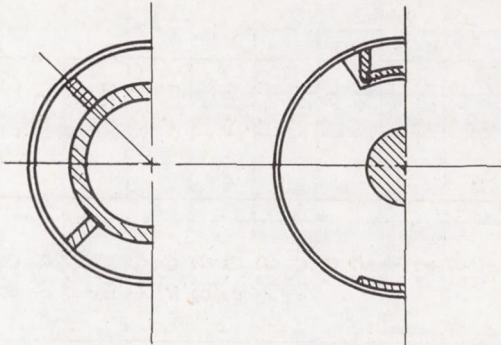
Figure 1. - Schematic diagram of elevation view of model. (All dimensions are in inches.)
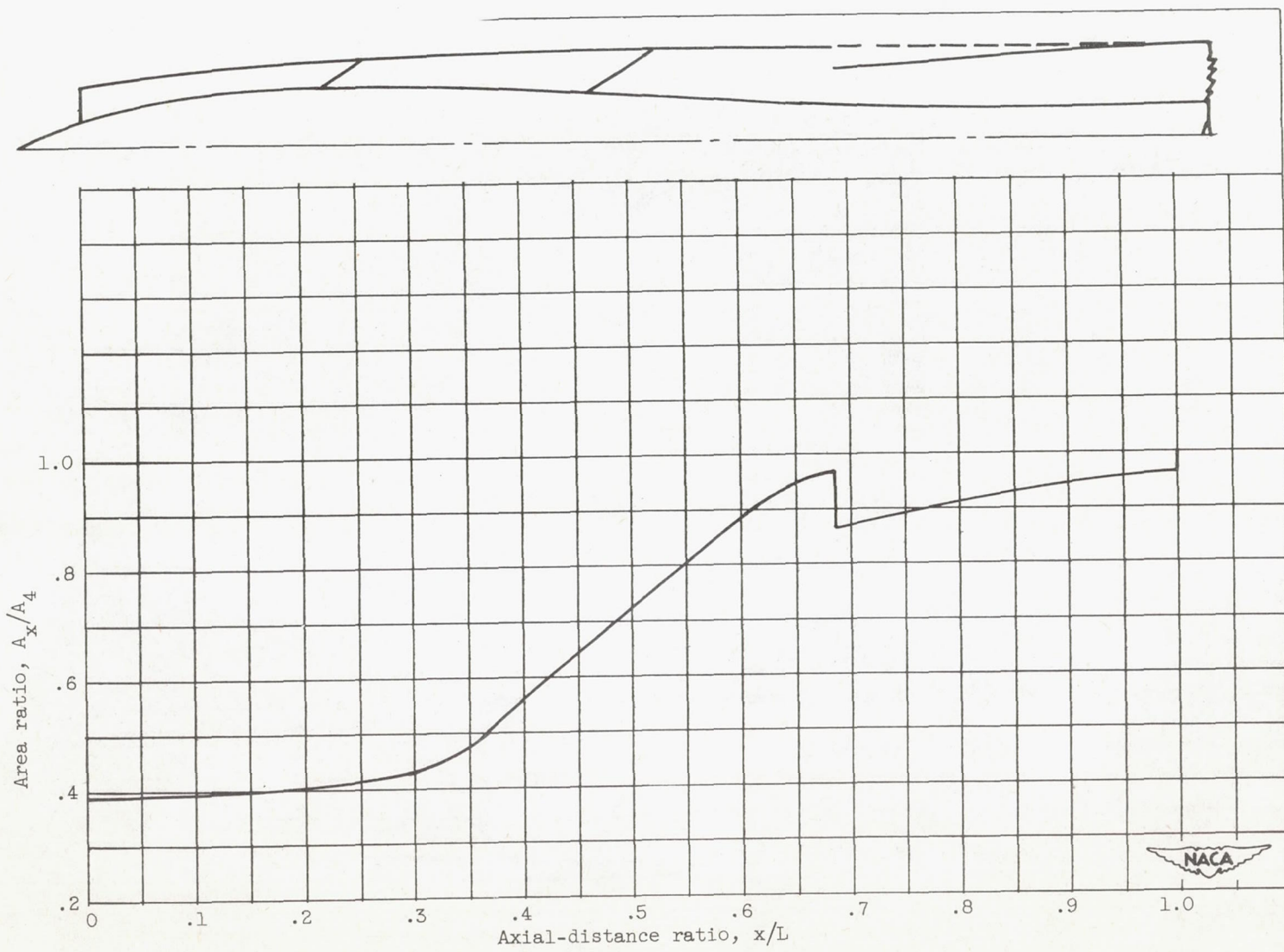
Figure 2. - Subsonic-diffuser area variation.
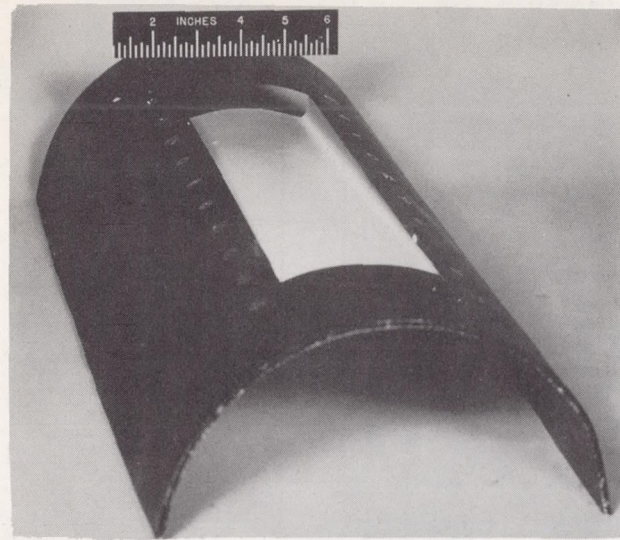
(a) External view (looking forward).

(b) Internal view (looking aft).
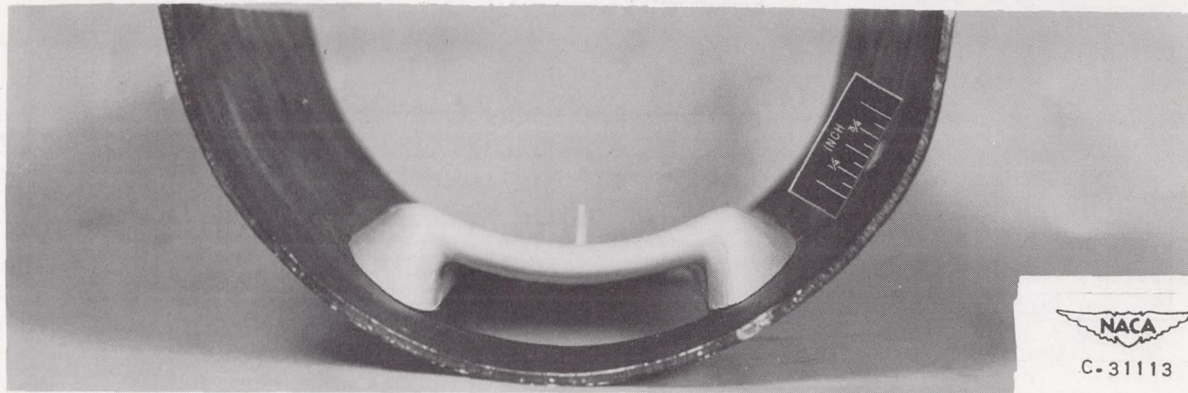
(c) Front view (looking aft).

Figure 3. - Photographs of bypass.

x	y	z	Flow area
0	3.63	0.94	3.50
.2	3.30	.788	2.62
.4	3.18	.712	2.40
.6	3.08	.660	2.22
.8	3.02	.627	2.03
.9	3.02	.618	1.90
1.0	3.02	.604	1.82
1.25	3.02	.650	1.97
1.64	3.02	.700	2.07

Section A-A

Station
32.0
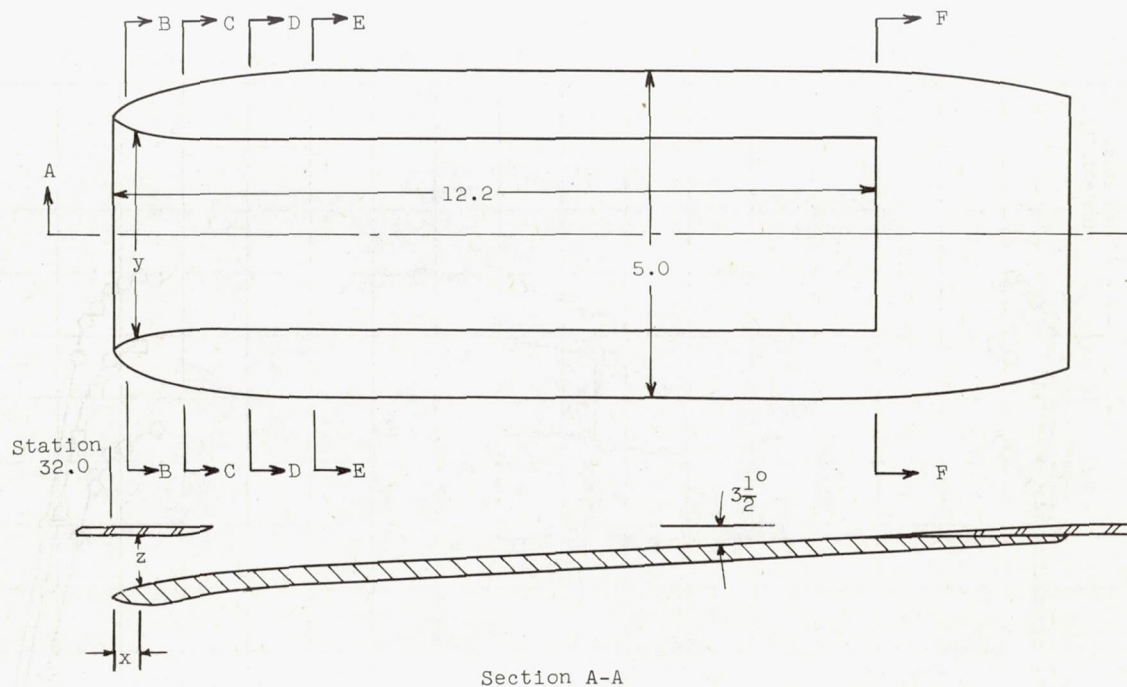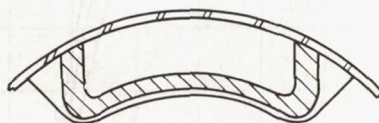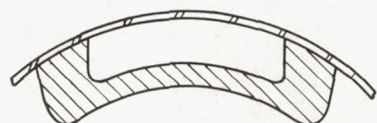
Section B-B

Section C-C
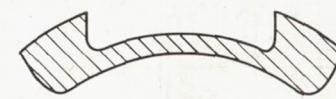
Section D-D
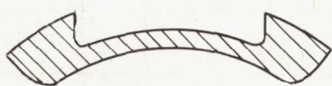
Section E-E
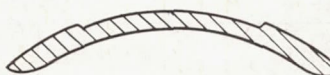
Section F-F
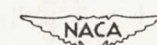
Figure 4. - Details of axial-discharge bypass. (All dimensions in inches.)
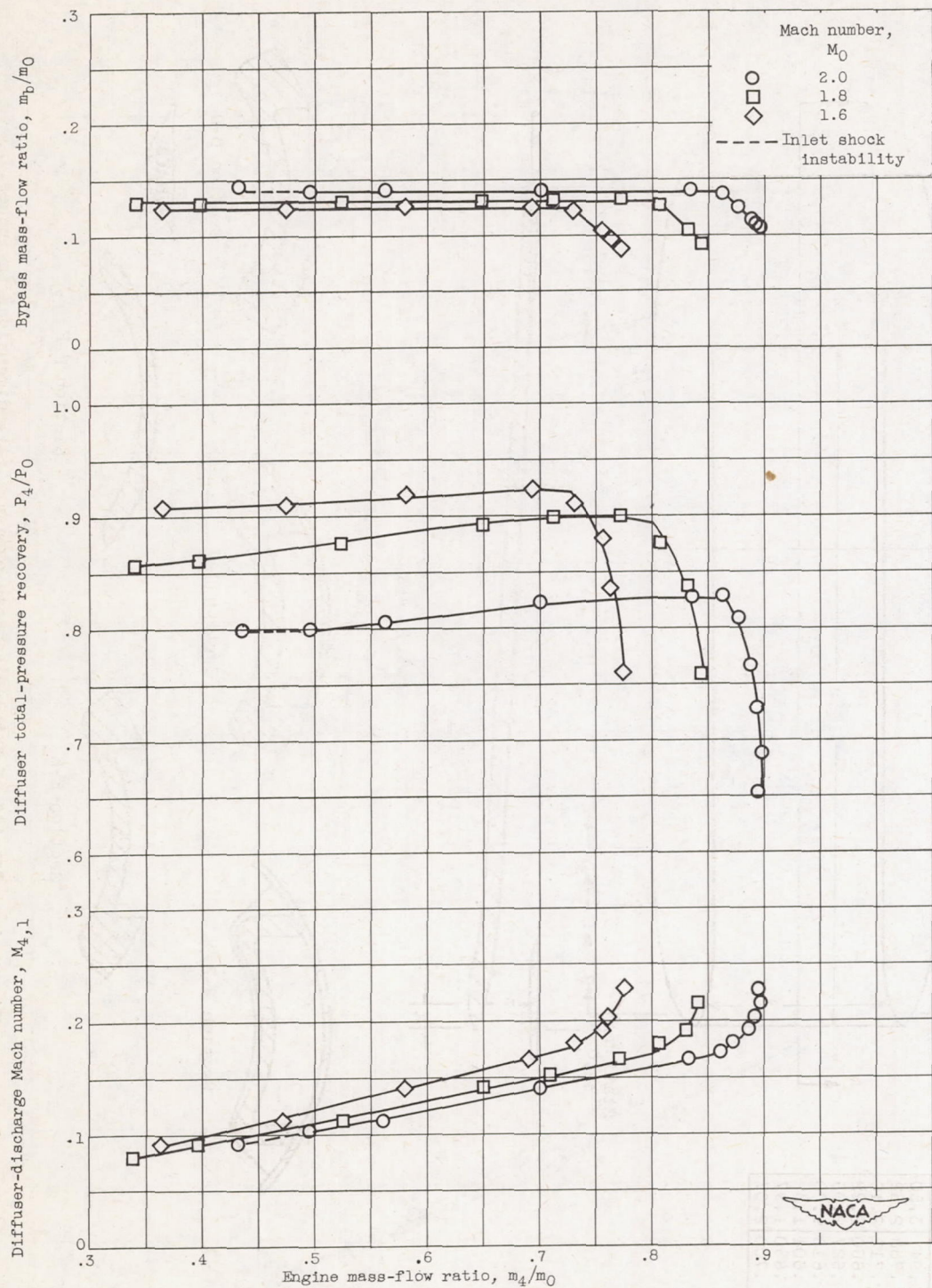
(a) Inlet characteristics.

Figure 5. - Variation of inlet characteristics and force coefficients with mass-flow ratio at zero nominal angle of attack for range of Mach numbers. Model with bypass on top.
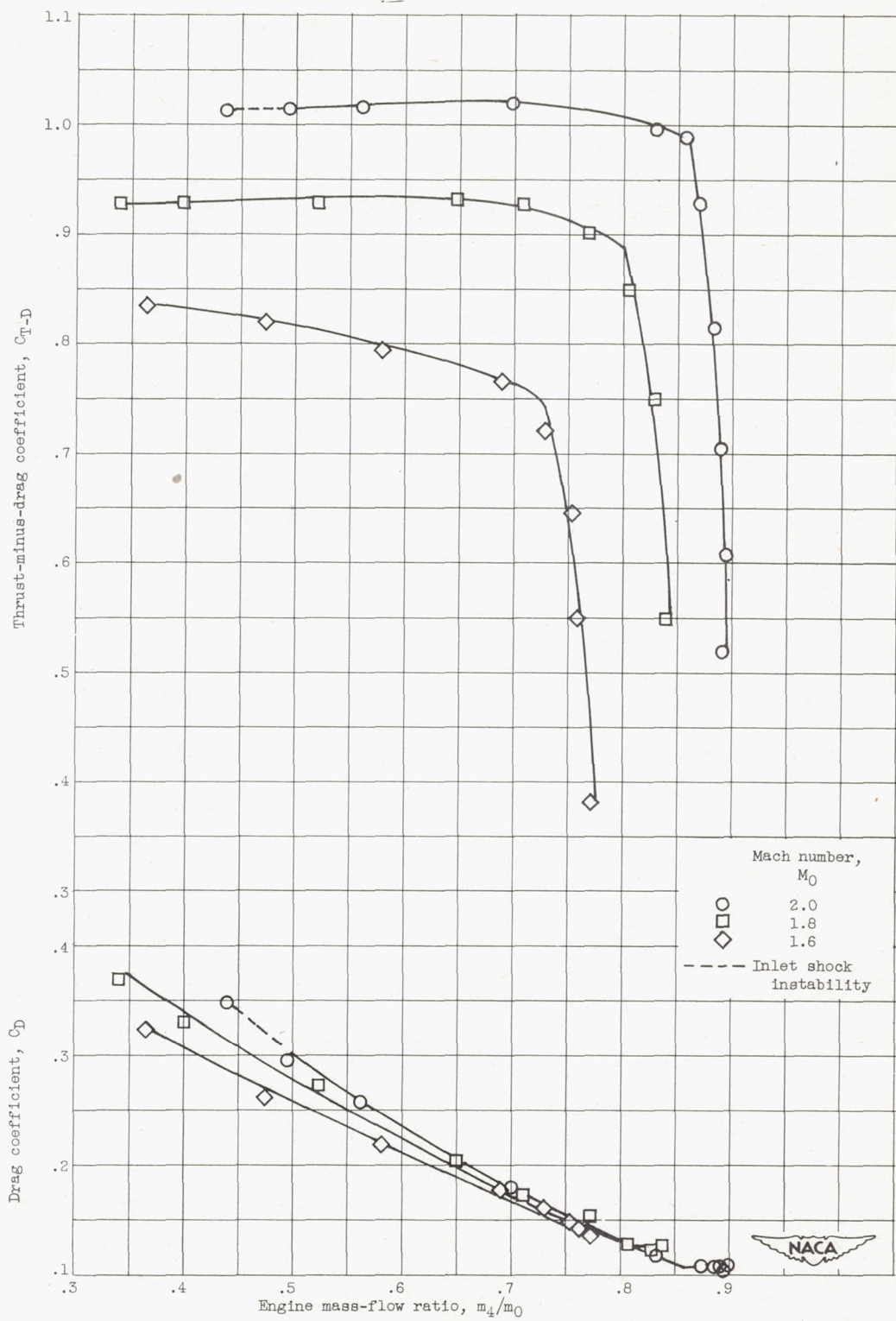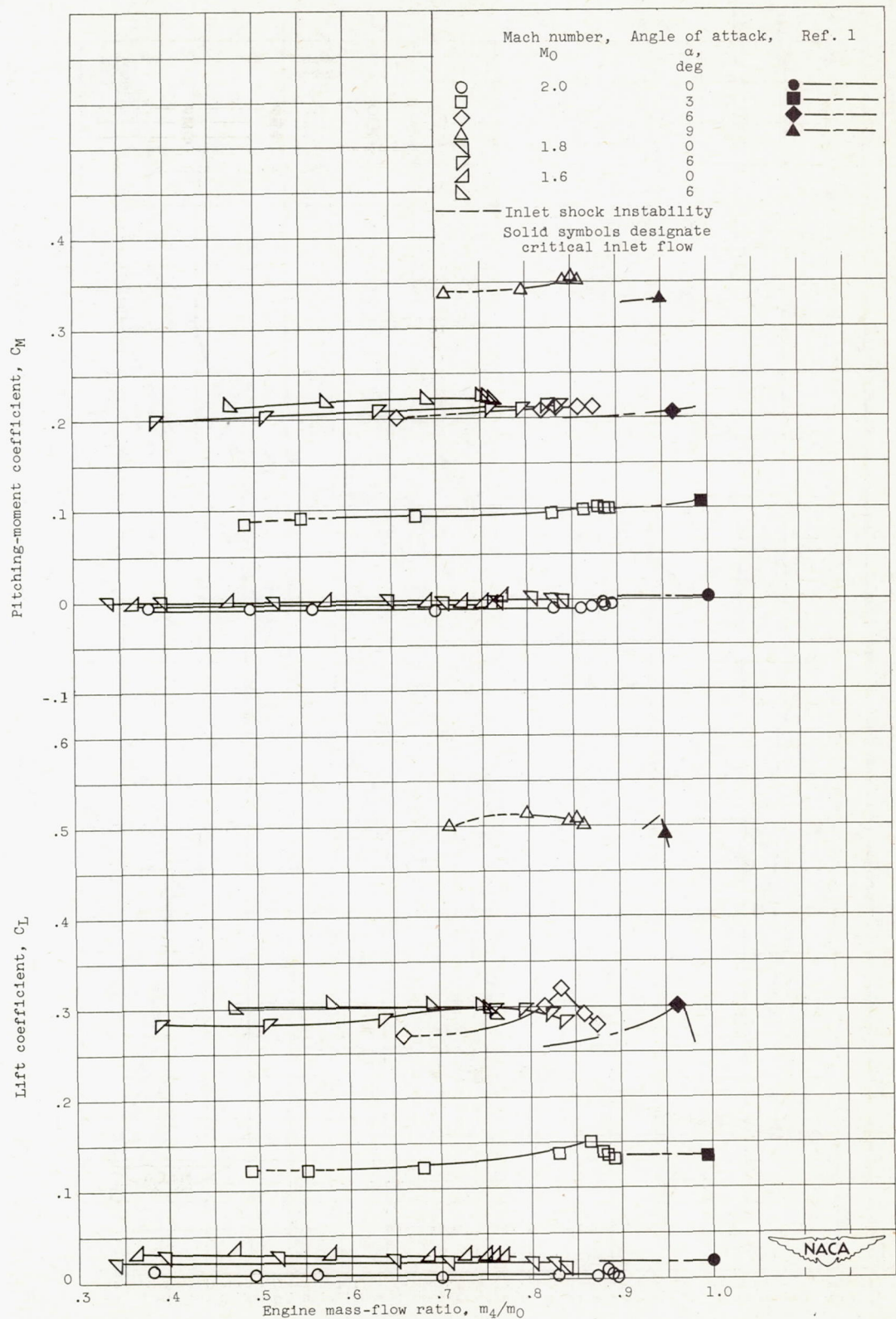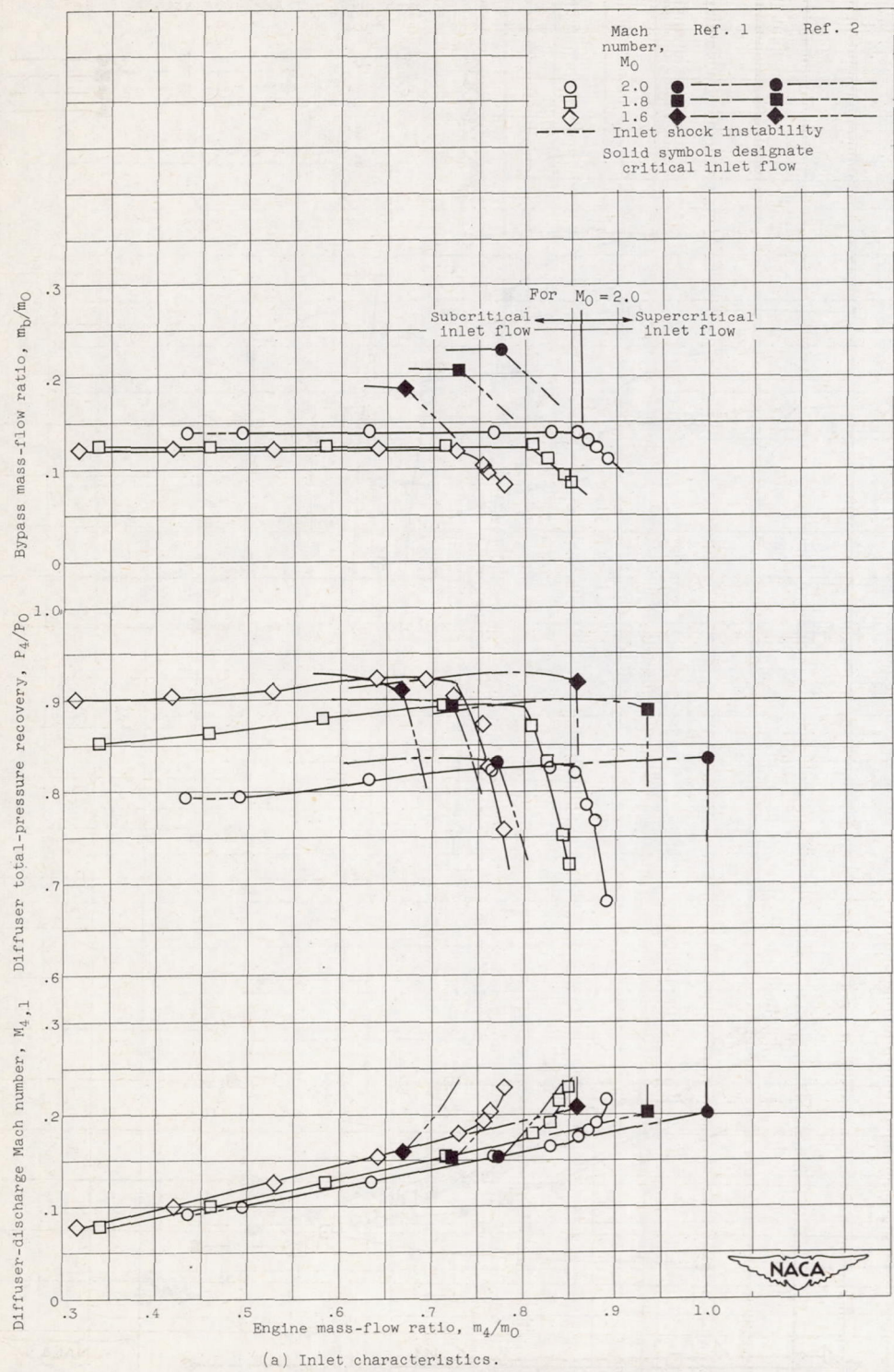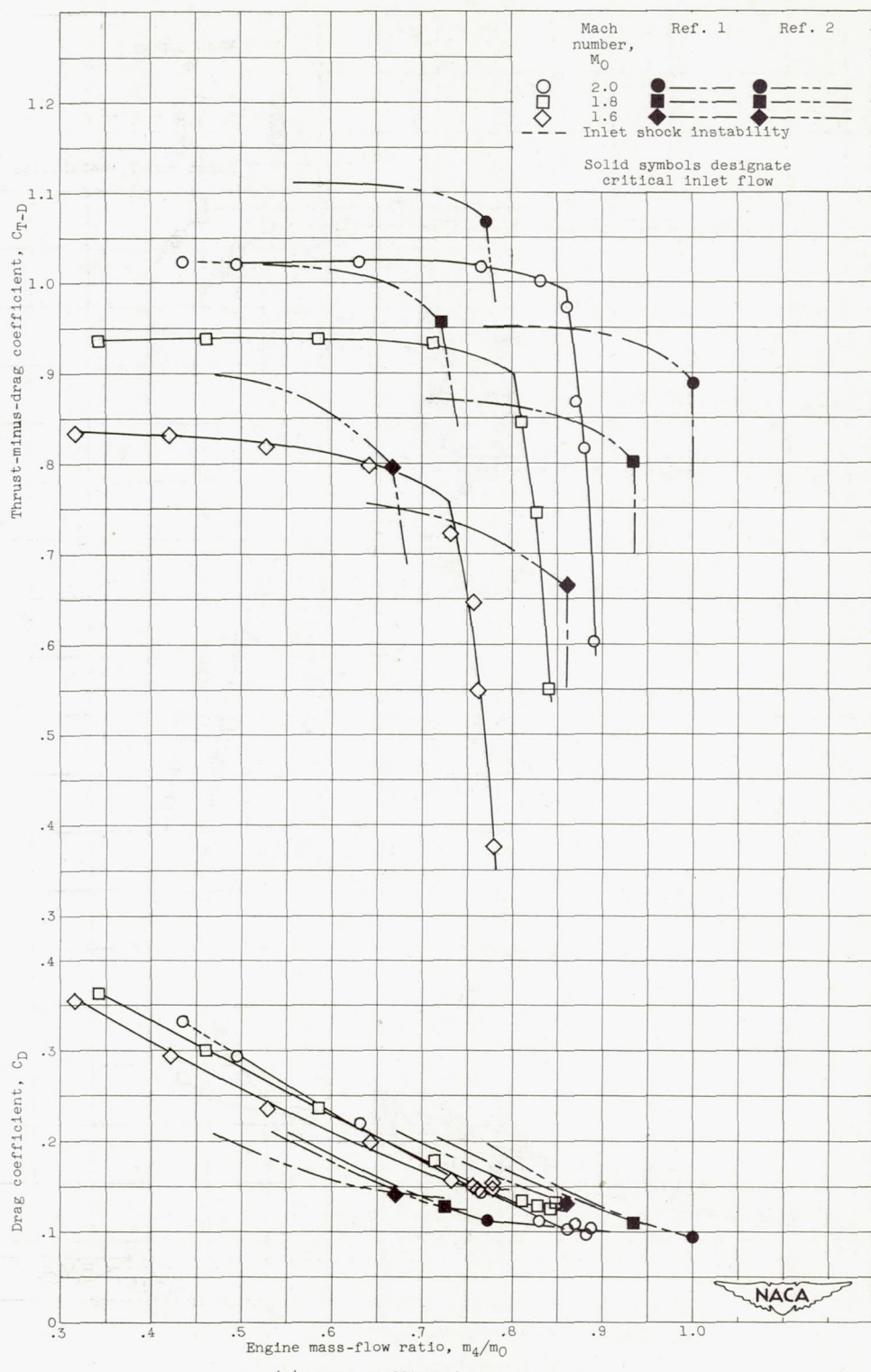
(b) Force coefficients.

Figure 5. - Concluded. Variation of inlet characteristics and force coefficients with mass-flow
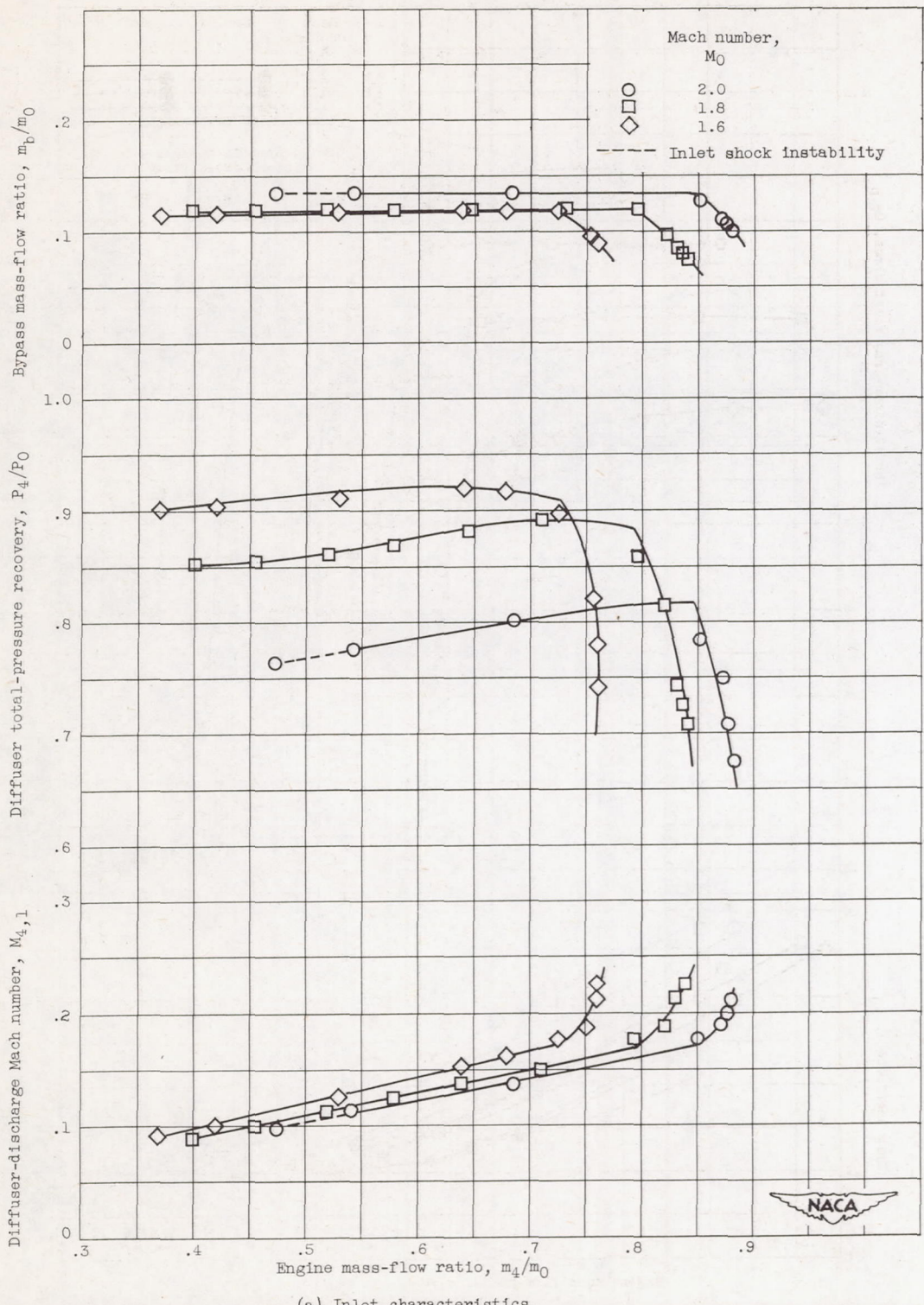ratio at zero nominal angle of attack for range of Mach numbers. Model with bypass on top.
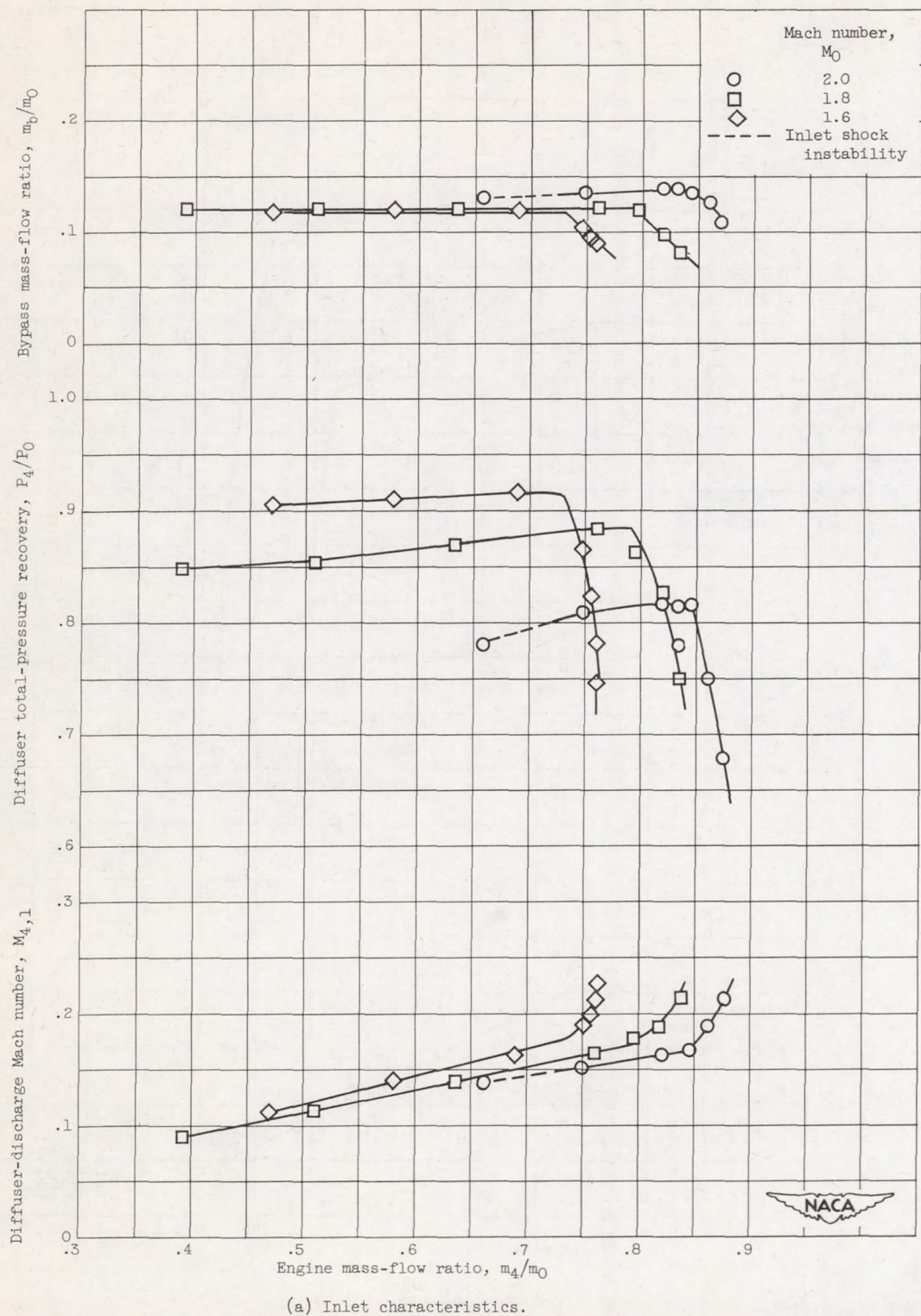
(a) Inlet characteristics.

Figure 6. - Variation of inlet characteristics and force coefficients with mass-flow ratio at nominal angle of attack of 6° for range of Mach numbers. Model with bypass on top.
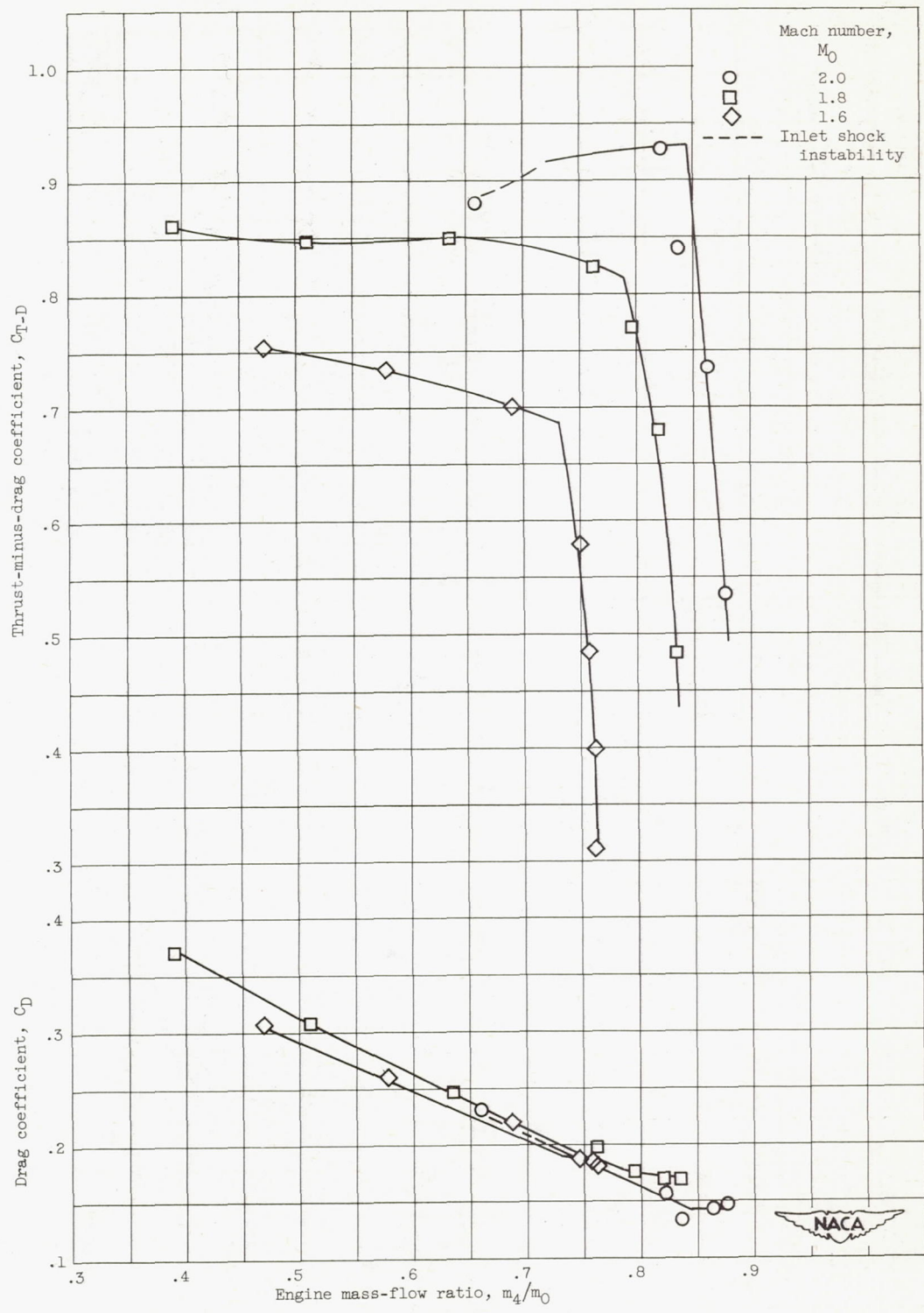
(b) Force coefficients.

Figure 6. - Concluded. Variation of inlet characteristics and force coefficients with mass-
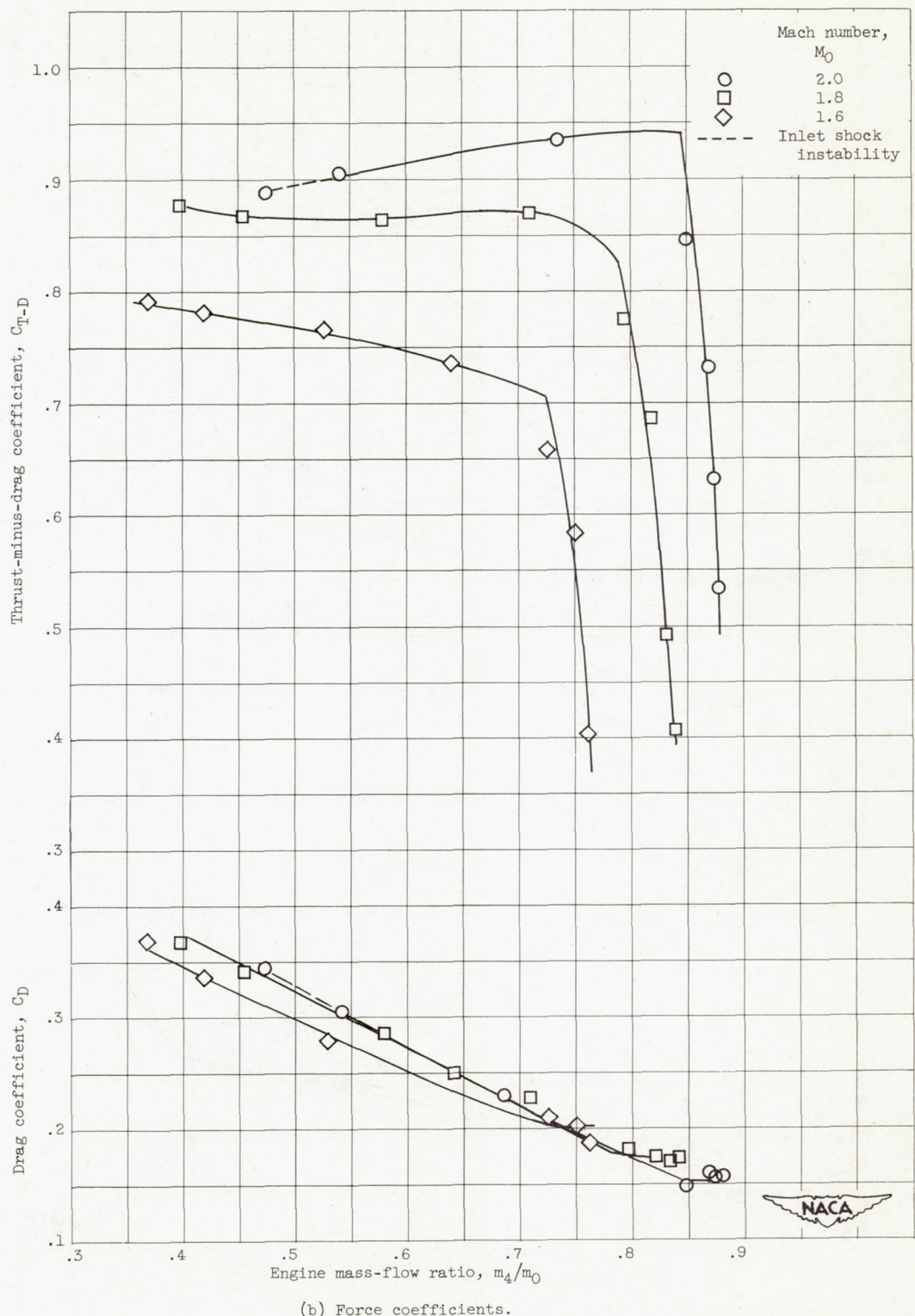flow ratio at nominal angle of attack of 6° for range of Mach numbers. Model with bypass
on top.
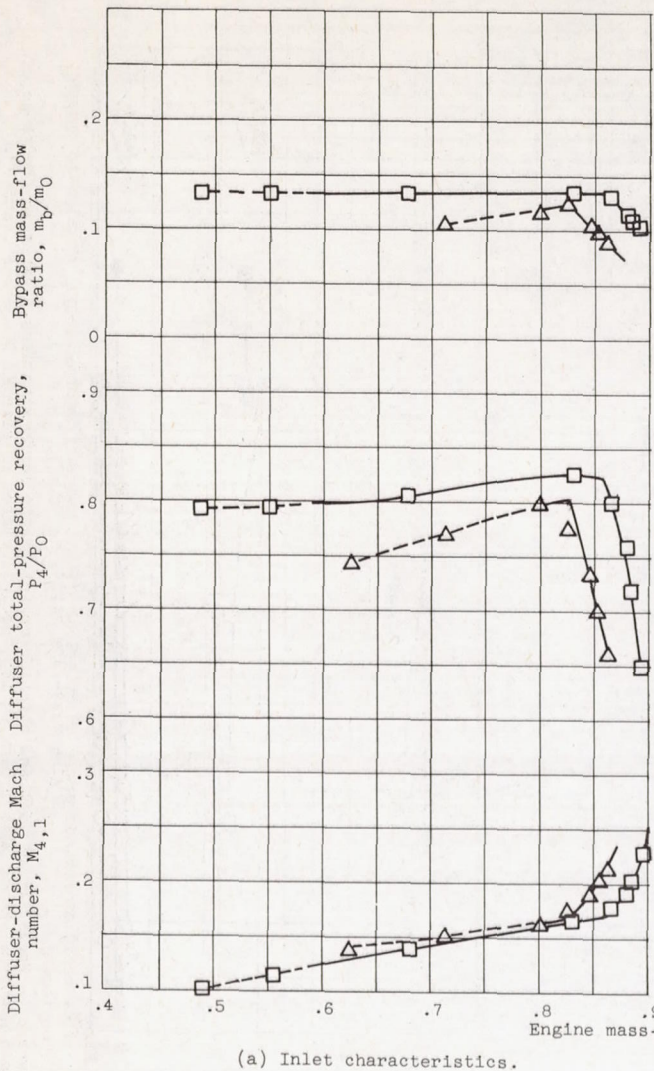
(a) Inlet characteristics.
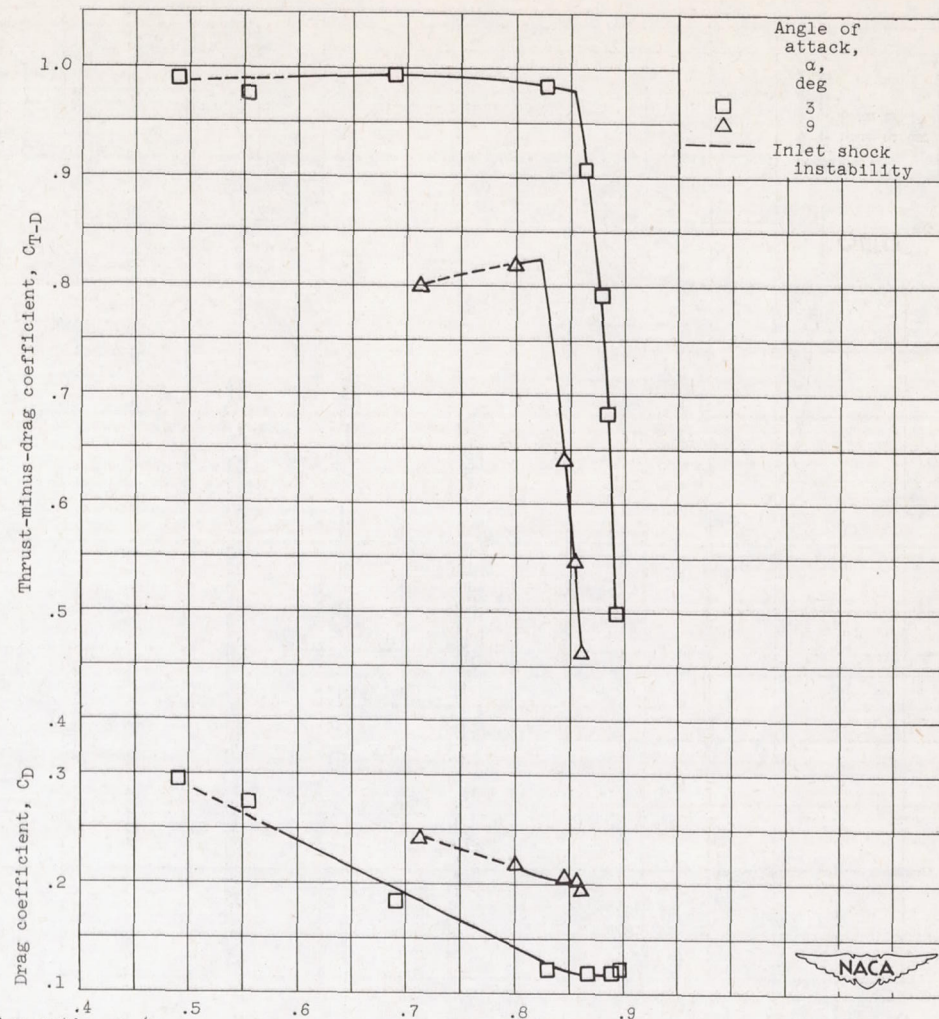
(b) Force coefficients.

Figure 7. - Variation of inlet characteristics and force coefficients with mass-flow ratio at nominal angles of attack of 3° and 9° for Mach number of 2.0. Model with bypass on top.

Figure 8. - Variation of lift and pitching-moment coefficients with mass-flow ratio for range of Mach numbers. Model with bypass on top, nominal angles of attack, 0°, 3°, 6°, and 9°.

(a) Inlet characteristics.

Figure 9. - Variation of inlet characteristics and force coefficients with mass-flow ratio at zero nominal angle of attack for range of Mach numbers. Model with bypass on bottom.

(b) Force coefficients.

Figure 9. - Concluded. Variation of inlet characteristics and force coefficients with mass-flow ratio at zero nominal angle of attack for range of Mach numbers. Model with bypass on bottom.
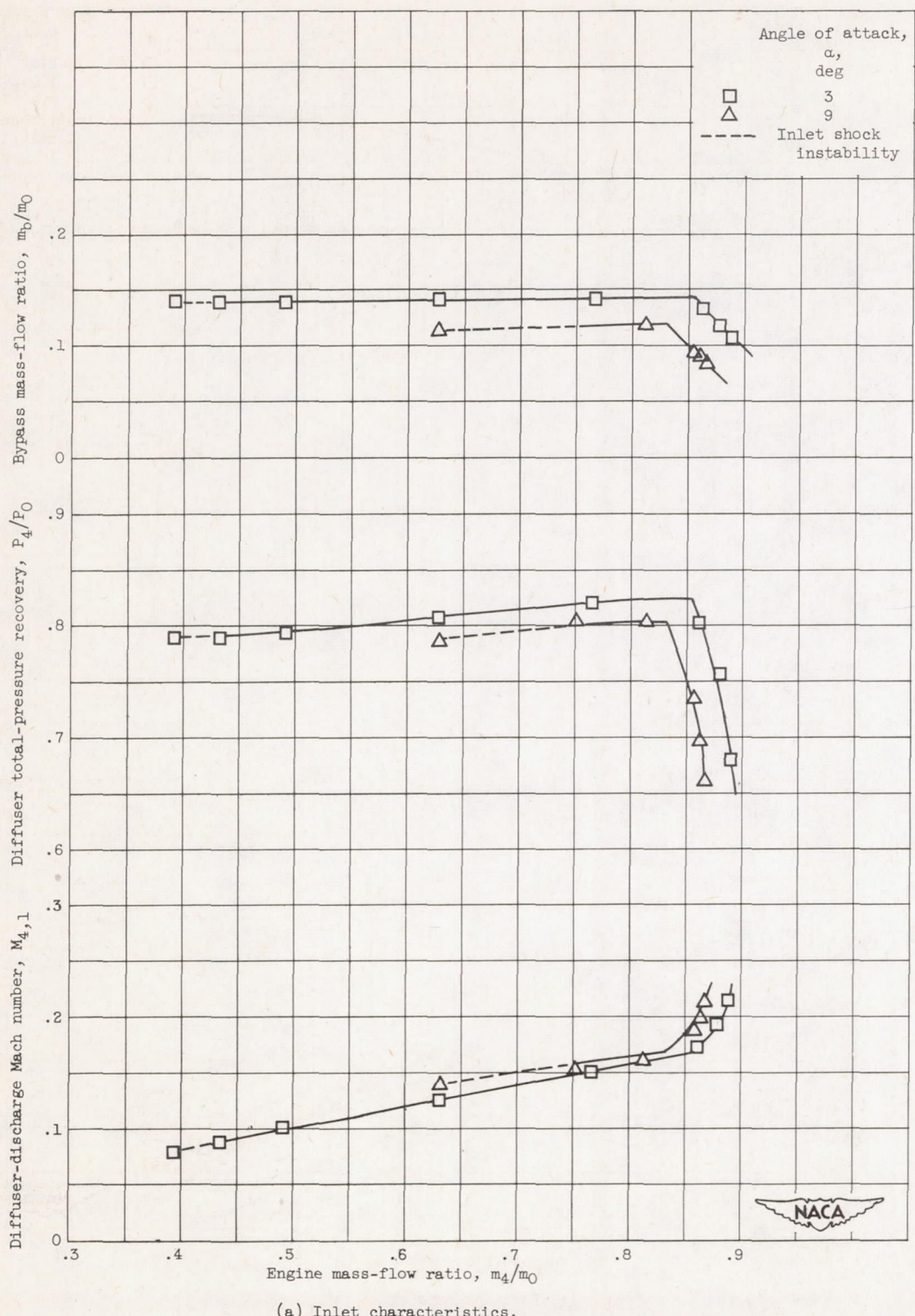
(a) Inlet characteristics.

Figure 10. - Variation of inlet characteristics and force coefficients with mass-flow ratio at nominal angle of attack of 6° for range of Mach numbers. Model with bypass on bottom.

(b) Force coefficients.

Figure 10. - Concluded. Variation of inlet characteristics and force coefficients with mass-
flow ratio at nominal angle of attack of 6° for range of Mach numbers. Model with bypass on
bottom.

(a) Inlet characteristics.

Figure 11. - Variation of inlet characteristics and force coefficients with mass-flow ratio at nominal angles of attack of 3° and 9° for Mach number of 2.0.   Model with bypass on bottom.
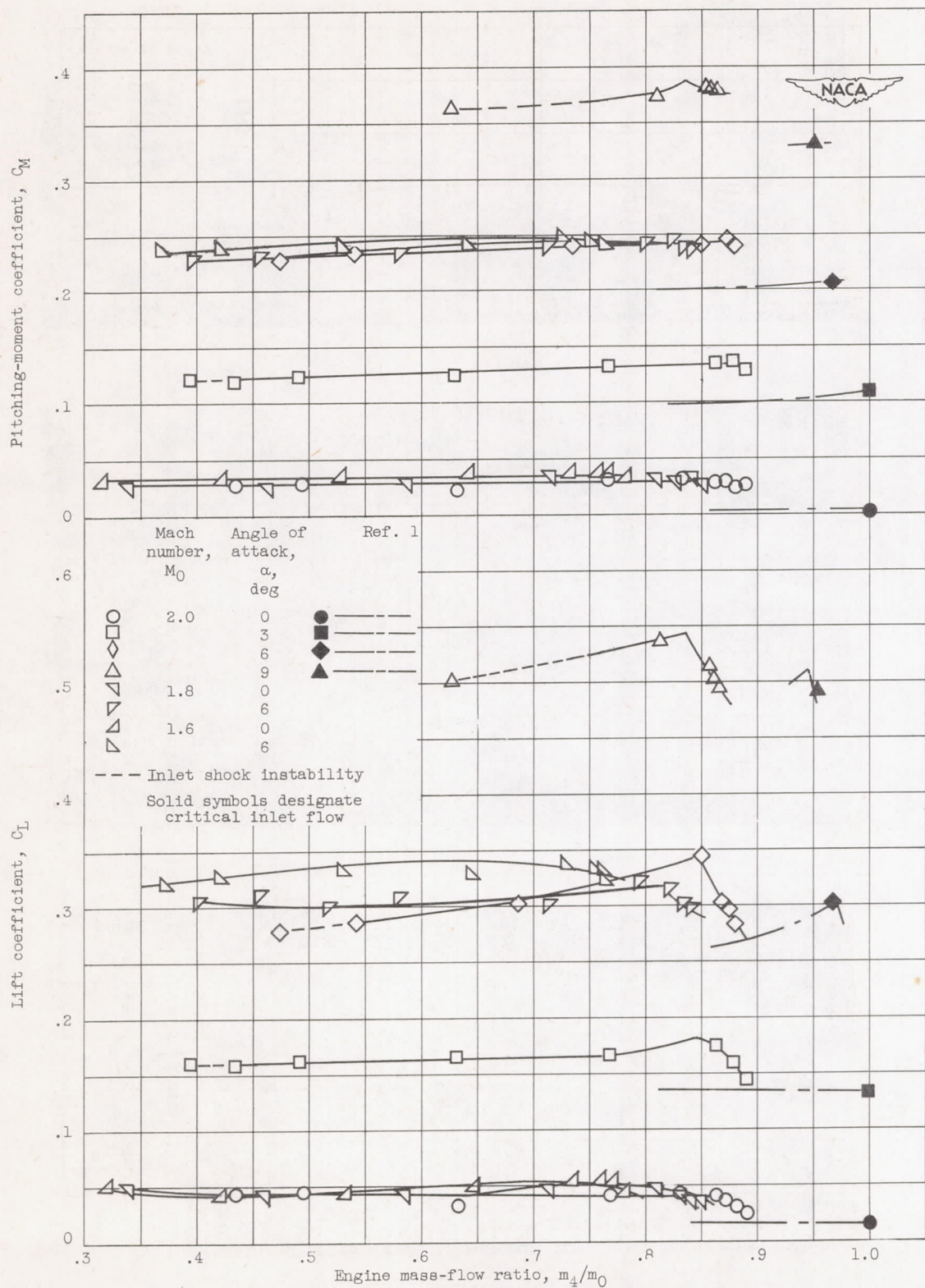
(b) Force coefficients.

Figure 11. - Concluded. Variation of inlet characteristics and force coefficients with mass-flow ratio at nominal angles of attack of 3° and 9° for Mach number of 2.0. Model with bypass on bottom.
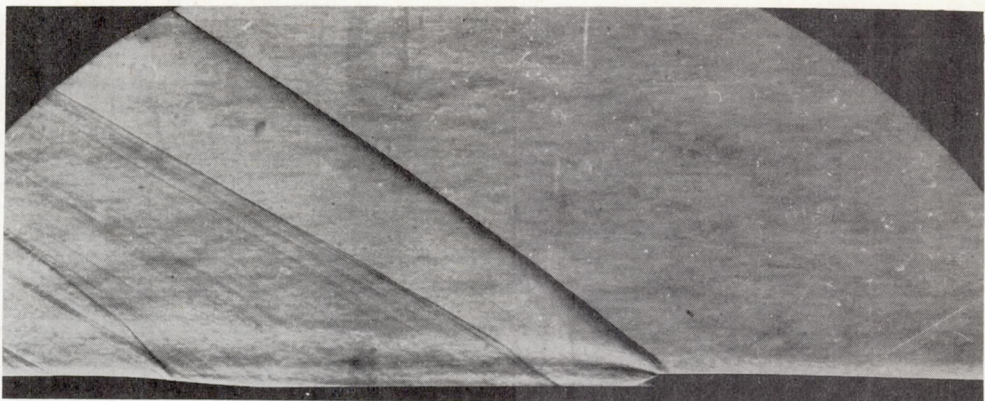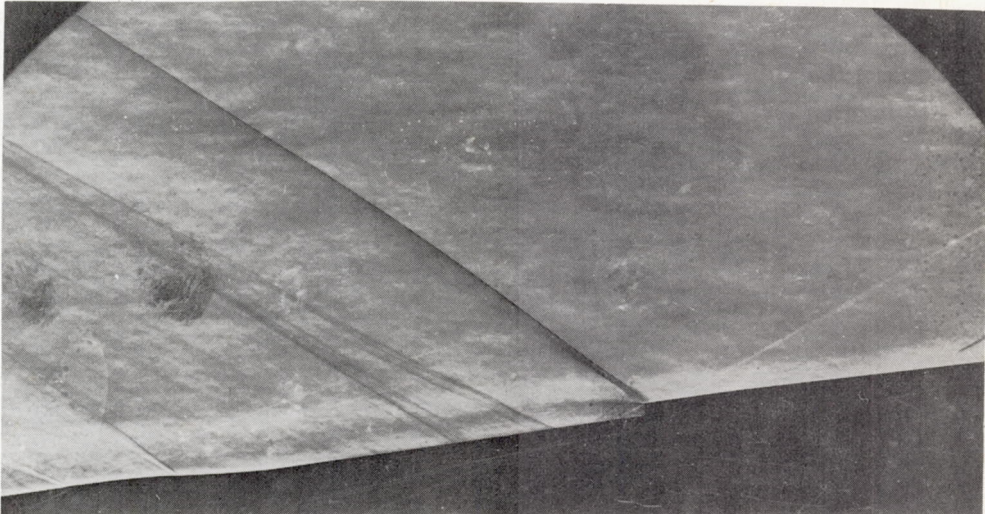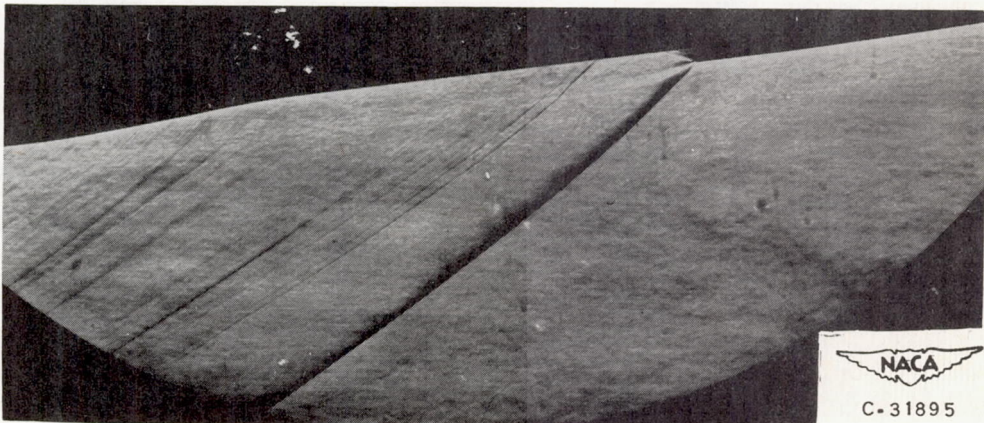
Figure 12. - Variation of lift and pitching-moment coefficients with mass-flow ratio for a range of Mach numbers. Model with bypass on bottom; nominal angles of attack, 0°, 3°, 6°, and 9°.

(a) $\alpha = 0^\circ$; $m_4/m_0 = 0.83$; $p_s/P_j = 0.17$.

(b) $\alpha = 9^\circ$; bypass on top; $m_4/m_0 = 0.80$; $p_s/P_j = 0.17$.

(c) $\alpha = 9^\circ$; bypass on bottom; $m_4/m_0 = 0.81$; $p_s/P_j = 0.18$.

Figure 13. - Schlieren photographs of bypass discharge at Mach number of 2.0.